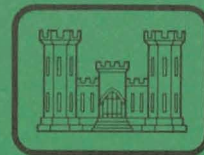


# Environmental & Water Quality Operational Studies



TECHNICAL REPORT E-80-5

## TRACER MEASUREMENT OF REAERATION: APPLICATION TO HYDRAULIC MODELS

Hydraulic Model Investigation

By Steven C. Wilhelms

Hydraulics Laboratory  
U. S. Army Engineer Waterways Experiment Station  
P. O. Box 631, Vicksburg, Miss. 39180

December 1980

Final Report

Approved for Public Release; Distribution Unlimited



Prepared for Office, Chief of Engineers, U. S. Army  
Washington, D. C. 20314

Under CWIS 31042  
(EWQOS Work Unit 31604 (IIIA.2))

Monitored by Environmental Laboratory  
U. S. Army Engineer Waterways Experiment Station  
P. O. Box 631, Vicksburg, Miss. 39180

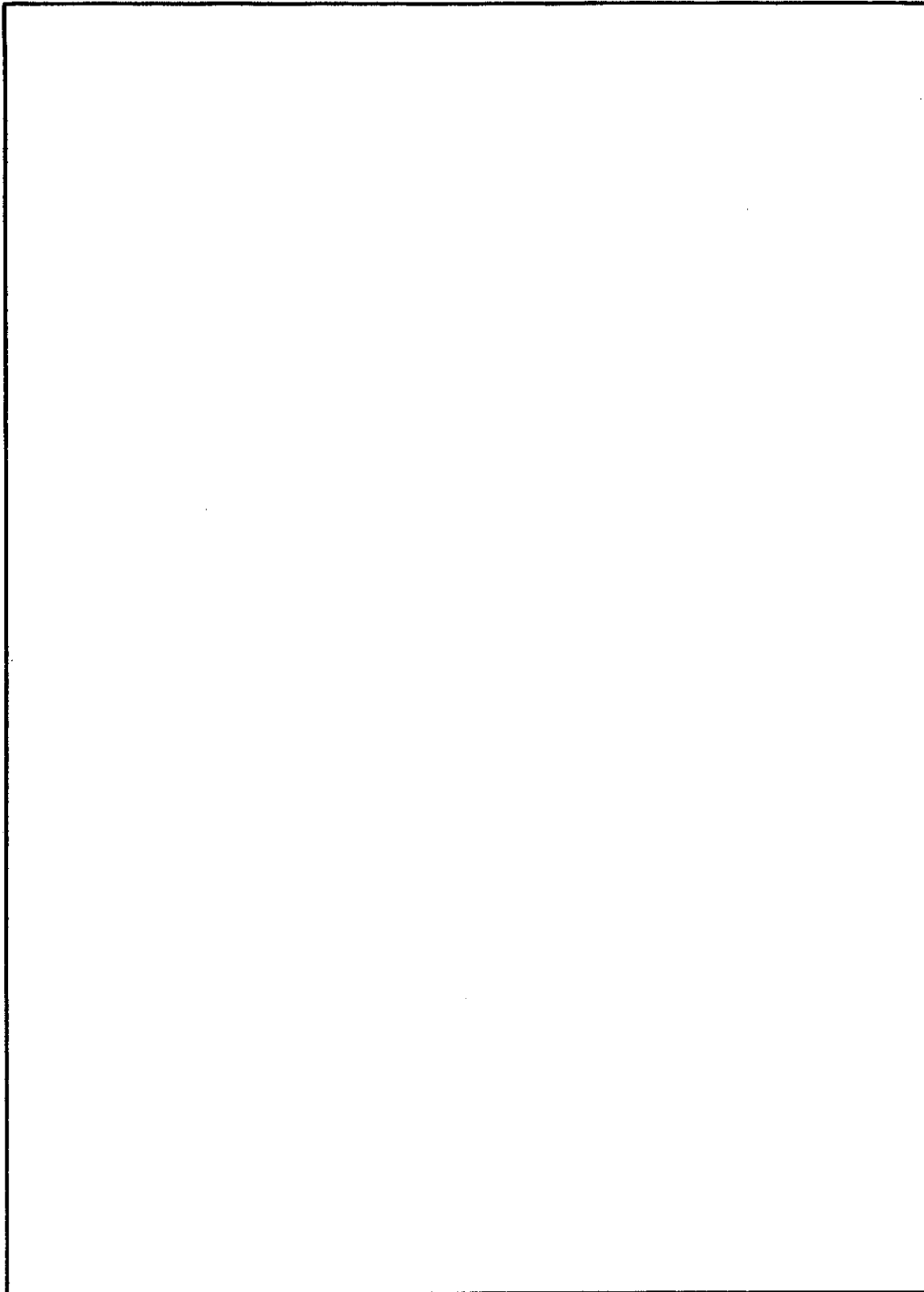


Unclassified

SECURITY CLASSIFICATION OF THIS PAGE (When Data Entered)

REPORT DOCUMENTATION PAGE		READ INSTRUCTIONS BEFORE COMPLETING FORM
1. REPORT NUMBER Technical Report E-80-5	2. GOVT ACCESSION NO.	3. RECIPIENT'S CATALOG NUMBER
4. TITLE (and Subtitle) TRACER MEASUREMENT OF REAERATION: APPLICATION TO HYDRAULIC MODELS; Hydraulic Model Investigation		5. TYPE OF REPORT & PERIOD COVERED Final report
		6. PERFORMING ORG. REPORT NUMBER
7. AUTHOR(s) Steven C. Wilhelms		8. CONTRACT OR GRANT NUMBER(s)
9. PERFORMING ORGANIZATION NAME AND ADDRESS U. S. Army Engineer Waterways Experiment Station Hydraulics Laboratory P. O. Box 631, Vicksburg, Miss. 39180		10. PROGRAM ELEMENT, PROJECT, TASK AREA & WORK UNIT NUMBERS CWIS No. 31042 (EWQOS Work Unit No. 31604 (IIIA.2))
11. CONTROLLING OFFICE NAME AND ADDRESS Office, Chief of Engineers, U. S. Army Washington, D. C. 20314		12. REPORT DATE December 1980
14. MONITORING AGENCY NAME & ADDRESS (if different from Controlling Office) U. S. Army Engineer Waterways Experiment Station Environmental Laboratory P. O. Box 631, Vicksburg, Miss. 39180		13. NUMBER OF PAGES 51
		15. SECURITY CLASS. (of this report) Unclassified
16. DISTRIBUTION STATEMENT (of this Report)  Approved for public release; distribution unlimited.		15a. DECLASSIFICATION/DOWNGRADING SCHEDULE
17. DISTRIBUTION STATEMENT (of the abstract entered in Block 20, if different from Report)		
18. SUPPLEMENTARY NOTES		
19. KEY WORDS (Continue on reverse side if necessary and identify by block number) Hydraulic models Radioactive tracers Reaeration Tracers		
20. ABSTRACT (Continue on reverse side if necessary and identify by block number)  This study presents the results of applying a gas tracer technique to determine the reaeration rate of flow through a hydraulic model. Radioactive tracers, krypton-85 and tritium, were used to determine the reaeration characteristics of two different spillway designs. The technique was sufficiently sensitive to detect gas-transfer changes due to the design changes tested. Dissolved oxygen (DO) uptake was predicted with results from the tracer tests and compared favorably with observed DO uptake from disturbed-equilibrium tests.		

**SECURITY CLASSIFICATION OF THIS PAGE(When Data Entered)**



**SECURITY CLASSIFICATION OF THIS PAGE(When Data Entered)**

## PREFACE

This investigation was conducted by the U. S. Army Engineer Waterways Experiment Station (WES), Hydraulics Laboratory (HL), from October 1976 to October 1977 under the direction of Messrs. H. B. Simmons, Chief of the HL, and J. L. Grace, Jr., Chief of the Hydraulic Structures Division. This effort was supported by a work unit (CWIS No. 31042) entitled "Methods of Enhancing Water Quality" of the Civil Works General Investigations, Environmental Quality Research Area and Reservoir Water Quality Research program sponsored by the Office, Chief of Engineers. This report was published under the Environmental and Water Quality Studies (EWQOS) program. Dr. J. L. Mahloch, Environmental Laboratory, was Program Manager of EWQOS.

The tests were conducted under the supervision of Mr. D. G. Fontane, former Chief of the Reservoir Water Quality Branch, and Dr. E. C. Tsivoglou, Consultant. Mr. Steven C. Wilhelms, in partial fulfillment of the requirements for a Master of Science degree, Civil Engineering, Mississippi State University (MSU), conducted the tests and prepared this report. Assisting in the testing and analysis were Ms. Cheryl Stevens of Dr. Tsivoglou's staff and Messrs. M. S. Dortch, C. H. Tate, B. Loftis, D. H. Merritt, and M. E. Neumann, all of the Hydraulic Structures Division, HL. Dr. V. L. Zitta of MSU provided guidance and technical assistance on the preparation and presentation of this report.

COL John L. Cannon, CE, and COL Nelson P. Conover, CE, were Commanders and Directors of WES during this investigation and report preparation. Mr. Fred R. Brown was Technical Director.

This report should be cited as follows:

Wilhelms, S. C. 1980. "Tracer Measurement of Reaeration: Application to Hydraulic Models; Hydraulic Model Investigation," Technical Report E-80-5, U. S. Army Engineer Waterways Experiment Station, CE, Vicksburg, Miss.

## CONTENTS

	<u>Page</u>
PREFACE . . . . .	1
PART I: INTRODUCTION . . . . .	4
Background . . . . .	4
Objective . . . . .	6
Scope . . . . .	6
PART II: RELEVANT THEORY . . . . .	7
Physics of Reaeration . . . . .	7
Other Theories of Gas Transfer . . . . .	12
Predictive Models of Reaeration . . . . .	14
Remarks . . . . .	17
PART III: METHODOLOGY . . . . .	18
Alternatives to the Tracer Technique . . . . .	18
Tracer Technique . . . . .	18
Model Facility . . . . .	22
PART IV: TESTING . . . . .	28
Apparatus and Equipment . . . . .	28
Procedure . . . . .	29
Analysis . . . . .	31
DO Uptake Tests . . . . .	33
PART V: RESULTS . . . . .	34
PART VI: CONCLUSIONS . . . . .	39
PART VII: RECOMMENDATIONS . . . . .	40
REFERENCES . . . . .	41
PLATES 1-8	

LIST OF FIGURES

No.		<u>Page</u>
1	Diffusion in quiescent water . . . . .	7
2	Diffusion and dispersion, effect of turbulent mixing . . .	10
3	Turbulent velocity . . . . .	11
4	Model facilities . . . . .	23
5	Spillway face without (top) and with (bottom) flip lip . .	24
6	Flow conditions with flip lip . . . . .	25
7	Flow conditions without flip lip . . . . .	26
8	High speed sampling system . . . . .	28
9	Sampling collection bottle . . . . .	29
10	Sampling system schematic . . . . .	30
11	Sampling station location . . . . .	31
12	Dose IV dye curve . . . . .	32
13	Predicted DO versus observed DO . . . . .	38

LIST OF TABLES

1	Empirical Prediction Models . . . . .	16
2	Semiempirical Prediction Models . . . . .	16
3	Krypton-to-Tritium, Ratios for All Tests . . . . .	35
4	Samples Used in $K_{kr}$ Analysis and Travel Time . . . . .	36
5	Test Summary . . . . .	37

# TRACER MEASUREMENT OF REAERATION: APPLICATION TO HYDRAULIC MODELS

## Hydraulic Model Investigation

### PART I: INTRODUCTION

#### Background

1. Man must have a clean, high quality water supply for personal consumption, growing food, and processing raw materials. Two major sources of water are rivers and lakes, thus the maintenance of high quality in these resources is of paramount importance. Clean, high quality water is the most important element to aquatic life also, since many kinds of life cannot survive in low quality or polluted water.

2. Oxygen is the one necessary element for survival of nearly all life forms. Low concentrations of oxygen in the aquatic environment is a hazardous condition for many kinds of life that exist there. Low dissolved oxygen (DO) in rivers and lakes is caused by the natural biological processes of assimilating organic material. It is important to note that streams, because of their movement, are well mixed and reaerate with oxygen from the atmosphere.

3. Consider a lake in early spring; the water is isothermal with a constant DO content from surface to bottom. As summer approaches, solar energy stratifies the lake into a warm upper region, the epilimnion, and a cold lower region, the hypolimnion. Wind, which had been mixing the entire lake under isothermal conditions and causing oxygen to be distributed throughout the water body, can now only mix the epilimnion since the hypolimnion is cold and heavy and remains in the lower levels of the lake. Organic material in the hypolimnion decomposes using oxygen and since mixing does not distribute atmospheric oxygen to the lower levels of the lake, the hypolimnion becomes low in DO or even anaerobic. Once this occurs it will usually remain until the late fall when cooling surface temperatures allow destratification and complete mixing of the water body.

4. Many man-made lakes release water through outlets located very deep in the lake. This results in low DO in the stream below the lake during the stratification season unless the release water is reaerated sufficiently to increase the oxygen content. There is great concern for providing adequate gas transfer to enhance the downstream DO. Thus it is extremely important to understand the gas transfer characteristics of the structures which release water from lakes, since it may be possible to build structures that promote gas transfer.

5. There are several numerical and experimental methods of evaluating oxygen uptake in streams and they are discussed in the next chapter. One method for accurately evaluating stream reaeration capacity was developed by the Federal Water Pollution Control Administration. A gaseous tracer,<sup>1</sup> which was the basis for the procedure, was first tested and demonstrated in one river,<sup>2</sup> and later applied in a series of direct field measurements<sup>3</sup> of stream reaeration. The development of the gaseous tracer technique marked a significant advance in the study of the reaeration process. The technique has been successfully applied to numerous streams<sup>4</sup> and is becoming accepted as one of the best methods<sup>5</sup> available for determining stream or river reaeration rates.

6. There are still many unanswered questions pertaining to reaeration or gas transfer. All of the field studies mentioned above have been on streams flowing in natural channels, with none in manmade structures such as stilling basins below dams, powerhouse tailraces, or other reservoir outlet works structures.

7. One method of determining the gas transfer characteristics of an existing structure is to use the tracer technique and test the prototype structure. However, this can be very costly and is not always possible. Modification of the stilling basins or energy dissipators to improve gas transfer characteristics of existing structures is usually very expensive. If the project is in the planning stage, then a prototype does not exist and accurate means of predicting gas transfer characteristics of proposed structures are not available. Because of these problems in evaluating the effects of design changes in hydraulic structures, it would be advantageous to test a hydraulic model of the

structure to determine its gas transfer characteristics and evaluate the effectiveness of alternate designs or structural modifications.

### Objective

8. The objective of this study was to demonstrate and evaluate the applicability of the tracer technique as a tool for use in physical models to determine gas transfer characteristics of hydraulic structures.

### Scope

9. Tests conducted in a physical hydraulic model of a spillway and stilling basin were used to evaluate the sensitivity of the tracer technique. Tests were conducted with and without a flip lip on the spillway to determine the ability of the technique to detect the effects of design modifications on gas transfer characteristics. Since reproducibility of results was of prime importance, two replicate tests were performed for such design (see Table 3 in Part IV).

## PART II: RELEVANT THEORY

### Physics of Reaeration

10. Reaeration can be considered as two processes working together, molecular diffusion and dispersion due to turbulent mixing. These are characterized by the capture of oxygen molecules from the atmosphere at the air/water interface and subsequent distribution of the oxygen throughout the volume of the water body. Molecular diffusion is caused by the inherent kinetic energy possessed by the oxygen molecules, whereas dispersion due to turbulent mixing results from the application of external forces on the volume elements of water.

11. If a group of dissolved molecules could be placed in a quiescent water body without disturbing the water, the dissolved molecules would gradually spread out through the water and eventually achieve a uniform distribution throughout the entire water body (Figure 1<sup>3</sup>). They would accomplish this in totally still water because of their own kinetic energy associated with their surrounding temperature. The average kinetic energy,  $KE$ , can be quantified as  $3/2 kT$ , where  $k$  is the Boltzmann constant and  $T$  is absolute temperature. In terms of mass and velocity, the kinetic energy is  $1/2 MV^2$  with  $V$  being an average velocity. The movement of the dissolved molecules, which is entirely

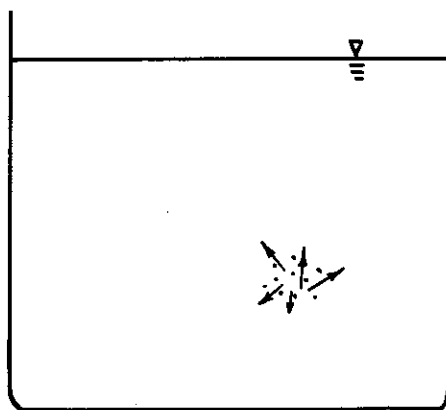


Figure 1. Diffusion in quiescent water

random, causes the molecules to uniformly distribute throughout the water body.

12. Fick's<sup>6</sup> first law quantifies the process of molecular diffusion:

$$J = -D_m \frac{dc}{ds} \quad (1)$$

where

$J$  = net flux of molecules across any plane in the water volume,

$$\frac{\text{gm}}{\text{sec} \cdot \text{cm}^2}$$

$D_m$  = coefficient of molecular diffusion,  $\text{cm}^2/\text{sec}$

$\frac{dc}{ds}$  = concentration gradient across the plane,  $\text{gm}/\text{cm}^3/\text{cm}$

The force driving molecular diffusion is the concentration gradient  $\frac{dc}{ds}$

where  $dc$  is the difference in molecule concentration on the two sides of the plane and  $ds$  is the infinitesimal distance from one side to the other.

13. Einstein<sup>7</sup> developed an expression for evaluating the molecular diffusion coefficient:

$$D_m = \frac{RT}{N_o f} \quad (2)$$

where

$R$  = universal gas constant,  $\text{gm} \cdot \text{cm}^2/\text{mole} \cdot \text{°K} \cdot \text{sec}^2$

$T$  = absolute temperature,  $\text{°K}$

$N_o$  = Avogadro's number,  $6.023 \times 10^{23}$  per mole

$f$  = friction factor,  $\text{gm}/\text{sec}$

The friction factor  $f$  is related to the ability of the surrounding medium to impede the movement of the diffusing molecules. Stokes<sup>8</sup> showed the friction factor to be directly related to the viscosity of the medium and the radius of spherical particles falling freely through the medium. Hence, the molecular diffusion coefficient is a function of the absolute temperature, viscosity of the fluid, and the size of the diffusing particle.

14. To further examine the molecular diffusion process related to gas transfer, consider a completely quiescent isothermal water body. Assume the water body is initially void of oxygen and the only source of oxygen molecules is the overlying atmosphere. A very short time later, oxygen molecules move into the surface layer of water because of their kinetic energy. The molecules move in random directions, thus, some escape back into the atmosphere while others move deeper into the fluid body. Since the diffusion downward is impeded by the viscosity of the water, the molecules tend to collect rapidly in the uppermost layers.

15. The net rate of gas molecule entry into the water is equal to the rate of entry from above (constant, because the overlying atmosphere has a constant oxygen partial pressure), minus the rate of escape back to the atmosphere (proportional to the dissolved oxygen partial pressure in the upper layers according to Henry's law<sup>9</sup>). Hence the rapid accumulation of gas molecules in the surface layers causes the net rate of entry to quickly become very small. According to Fick's law, the mass transfer rate through a plane is proportional to the concentration gradient across that plane. In this case the concentration gradient becomes very small resulting in a very small mass transfer rate across the air/water interface. Thus, the lower water volume elements are "starved" for oxygen.

16. Consider that same body of water with no dissolved oxygen and the only source of oxygen molecules being the overlying atmosphere. However, this time, the water is being agitated causing turbulent mixing (Figure 2). Turbulent mixing and convection cause water element 1 to come in contact with the atmosphere. The contact time may be very short but because the concentration gradient from the atmosphere to the volume element is large the rate of mass transfer is large (Fick's first law). Hence, element 1 acquires a relatively large amount of oxygen. The element is then swept away from the surface and comes in contact with volume element 2 which has no dissolved oxygen. Because the concentration gradient across the interface of elements 1 and 2 is large, the rate of mass transfer is large and element 2 acquires a significant amount of oxygen. All the volume elements in the water body multiply this

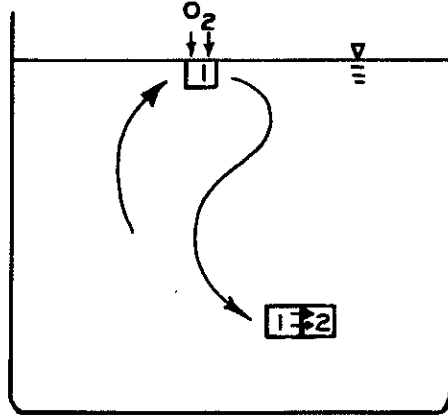


Figure 2. Diffusion and dispersion, effect of turbulent mixing

process; thus, it is obvious that dispersion caused by turbulent mixing greatly speeds gas transfer.

17. The turbulent mixing process and dispersion have been mathematically described by the following equation<sup>6,10</sup>

$$\frac{\partial c}{\partial t} + \frac{u\partial c}{\partial x} + \frac{v\partial c}{\partial y} + \frac{w\partial c}{\partial z} = D_m \left( \frac{\partial^2 c}{\partial x^2} + \frac{\partial^2 c}{\partial y^2} + \frac{\partial^2 c}{\partial z^2} \right) \quad (3)$$

where

$c$  = substance concentration, gm/cm<sup>3</sup>

$t$  = time, sec

$u$  = velocity in x-direction, cm/sec

$v$  = velocity in y-direction, cm/sec

$w$  = velocity in z-direction, cm/sec

$D_m$  = molecular diffusion coefficient, cm<sup>2</sup>/sec

In turbulent flow the velocities and concentration are expressed as a mean  $\bar{u}$  value plus a randomly fluctuating component  $u'$  (Figure 3).

18. For example, the velocity in the x-direction is  $u = \bar{u} + u'$ . Velocities in the y- and z-directions and concentration are expressed

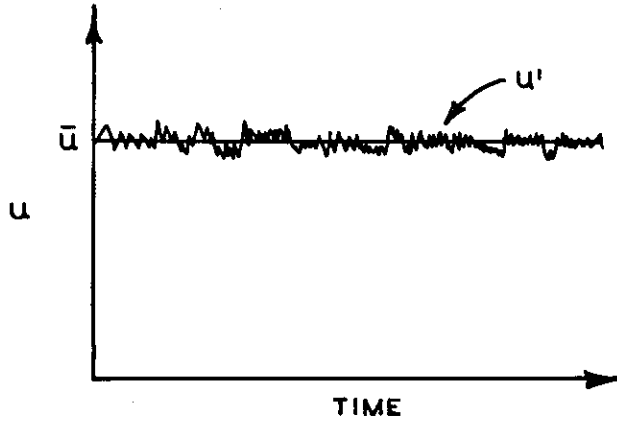


Figure 3. Turbulent velocity

similarly. Making these substitutions in Equation 3 and taking a time average of each term the following equation is obtained:

$$\begin{aligned} \frac{\partial \bar{c}}{\partial t} + \frac{\bar{u} \partial \bar{c}}{\partial x} + \frac{\bar{v} \partial \bar{c}}{\partial y} + \frac{\bar{w} \partial \bar{c}}{\partial z} + \frac{\partial (\overline{u'c'})}{\partial x} + \frac{\partial (\overline{v'c'})}{\partial y} + \frac{\partial (\overline{w'c'})}{\partial z} \\ = D_m \left( \frac{\partial^2 \bar{c}}{\partial x^2} + \frac{\partial^2 \bar{c}}{\partial y^2} + \frac{\partial^2 \bar{c}}{\partial z^2} \right) \end{aligned} \quad (4)$$

where the horizontal bar, i.e.  $\bar{u}$ ,  $\partial (\overline{u'c'})$ , denotes a time average.

The terms

$$\frac{\partial (\overline{u'c'})}{\partial x} + \frac{\partial (\overline{v'c'})}{\partial y} + \frac{\partial (\overline{w'c'})}{\partial z} \quad (5)$$

are the turbulent mass flux per unit area and are similar to "Reynolds stresses"

$$\frac{\partial (\overline{u'})^2}{\partial x} + \frac{\partial (\overline{u'v'})}{\partial y} + \frac{\partial (\overline{u'w'})}{\partial z} \quad (\text{x-direction}) \quad (6)$$

as found in the turbulent momentum transport equations.

19. Boussinesq<sup>10</sup> theorized that these stresses could be related linearly to the gradient of average velocity,

$$(\overline{u'v'}) = -\epsilon \frac{d\bar{u}}{dy} \quad (7)$$

where

$\varepsilon$  = turbulent exchange coefficient,  $\text{cm}^2/\text{sec}$

Similarly, and by analogy<sup>6</sup> with Fick's first law (Equation 1), those turbulent dispersion terms have been related to the gradient of average concentration,

$$\overline{(u'c')} = -E_x \frac{\partial \bar{c}}{\partial x} \quad (8)$$

where

$E_x$  = turbulent dispersion coefficient in x-direction,  $\text{cm}^2/\text{sec}$

20. The turbulent transport process equation can be written as

$$\begin{aligned} \frac{\partial \bar{c}}{\partial t} + \bar{u} \frac{\partial \bar{c}}{\partial x} + \bar{v} \frac{\partial \bar{c}}{\partial y} + \bar{w} \frac{\partial \bar{c}}{\partial z} = D_m \left( \frac{\partial^2 \bar{c}}{\partial x^2} + \frac{\partial^2 \bar{c}}{\partial y^2} + \frac{\partial^2 \bar{c}}{\partial z^2} \right) \\ + \frac{\partial}{\partial x} \left( E_x \frac{\partial \bar{c}}{\partial x} \right) + \frac{\partial}{\partial y} \left( E_y \frac{\partial \bar{c}}{\partial y} \right) + \frac{\partial}{\partial z} \left( E_z \frac{\partial \bar{c}}{\partial z} \right) \end{aligned} \quad (9)$$

In most turbulent flow, the dispersion coefficient,  $E$ , is much greater than the molecular diffusion coefficient,  $D_m$ . Thus, molecular diffusion typically limits the rate of reaeration. But turbulent dispersion and convection result in a very high rate of molecular diffusion at the surface at all times. Thus, the rate of reaeration is greatly dependent on turbulence and convection. Turbulence, in reference to reaeration, has a special meaning related to the rate of surface replacement and dispersion of water volume elements.

#### Other Theories of Gas Transfer

21. The preceding theory conflicts with the "two film" theory of gas transfer developed by Lewis and Whitman.<sup>11</sup> In a well-mixed system a stable saturated surface layer cannot exist; constant surface replacement precludes this. Danckwerts "surface renewal" theory<sup>12</sup> is more aligned with the theory discussed in previous paragraphs. According to Danckwerts, fluid elements are exposed to the atmosphere for varying periods of time and the chance of an element being swept back into the

fluid body and being replaced by another at the surface is independent of its "exposure time." He theorized that the rate of surface area renewal is constant for a given system. He surmised that the fraction of surface area with age between  $t$  and  $t + dt$  is equal to the fraction of surface area which previously had age between  $t$  and  $t - dt$  minus the portions which had been replaced in the time interval  $dt$ ; obtaining the distribution of fractional area to be

$$\theta(t) = re^{-rt} \quad (10)$$

where

$\theta(t)$  = fractional area distribution as a function of time, per sec

$r$  = surface renewal rate, per sec

22. According to this theory, the surface elements absorb oxygen molecules up to the instant they are swept away from the surface. Coupling this theory with Fick's law, the average absorption rate was determined to be a function of the surface renewal rate,  $r$ .

23. Dobbins<sup>13</sup> developed the "film-penetration" theory of gas transfer. He reasoned that the concentration gradient within the fluid body was negligible when compared to the gradient in the surface layer, hence the bulk concentration could be considered constant and the diffusion equation only applied at the surface. Dobbins adhered to the concept of a thin film whose elements absorbed gas by molecular diffusion before being replaced. He used the surface age distribution obtained by Danckwerts and determined that the average absorption rate of oxygen molecules was a function of the surface renewal rate and the thin film thickness.

24. These theories allow for increased gas transfer through increased surface renewal rates. They do not account for the increased mixing and molecular diffusion between water elements within the body of water upon which the reaeration rate is highly dependent. Further, in most complex natural or nonlaboratory systems, it is very difficult, if not impossible, to evaluate the surface renewal rate and the thin film thickness.

## Predictive Models of Reaeration

25. Numerous models have been developed for predicting the reaeration coefficient. Those models may be classified as theory-based, semi-empirical, or totally empirical. Theory-based models are developed from conceptual models of gas transfer. Semiempirical models relate the reaeration coefficient to the rate of energy dissipation or longitudinal dispersion. Totally empirical models relate the reaeration coefficient to the average flow velocity and average depth of flow.

26. The most well known theory-based prediction equation is the O'Connor-Dobbins<sup>14</sup> model. It was obtained from the derivation of Dobbins' "film penetration" theory of gas transfer and relates the rate of reaeration to the liquid film diffusion coefficient, mean forward velocity, average water depth, and channel slope by assuming that the surface renewal rate was equal to the inverse of the time scale of the vertically fluctuating velocity component,

$$r = \frac{v'}{\ell} \quad (11)$$

where

$v'$  = vertical velocity fluctuations, cm/sec

$\ell$  = mixing length, cm

Prandtl's definition of mixing length and a logarithmic velocity distribution provided a basis for evaluating the surface renewal rate in terms of the mean depth of flow, the channel slope, and the gravitational and Von-Karman constants. For a relatively deep channel with a presumably small velocity gradient, the surface renewal rate was related to the average forward velocity and the average depth of flow. The form of the model is

$$K_2 \propto \frac{\bar{V}^a}{H^b} \quad (12)$$

where

$K_2$  = reaeration rate coefficient for the stream, per sec

$\bar{V}$  = mean forward velocity, cm/sec

H = average depth of flow, cm

a,b = experimental constants

O'Connor and Dobbins determined that the constants, a and b, were 0.5 and 1.50, respectively.

27. Many of the empirical prediction equations have the same form as the O'Connor-Dobbins model, but with different exponents on the average velocity and average depth of flow. These models, such as Bennett-Rathbun,<sup>15</sup> Churchill, Elmore, and Buckingham,<sup>16</sup> Langbein and Durum,<sup>17</sup> and Bansal,<sup>18</sup> were developed using multiple linear regression and several hydraulic parameters of open channel flow. Average velocity, average width, mean depth, and channel slope are some of these parameters. Least squares criterion was the usual method of fitting the regression equation to the investigator's data.

28. Table 1 shows empirical model exponents indicating similarities and differences among models due to development with different data sets. The linear proportionality constant differs for each model also.

29. Semiempirical models such as Krenkel-Orlob,<sup>19</sup> Cadwallader-McDonnell,<sup>20</sup> and Tsivoglou-Wallace<sup>3</sup> relate the reaeration rate coefficient to the average forward velocity,  $\bar{V}$ , slope of the energy gradient, S, and mean depth of flow, H. The form of these models is

$$K_2 \propto \frac{(\bar{V}S)^a}{H^b} \quad (13)$$

Table 2 shows the exponent values for the above-mentioned models. The exponents differ again due to development with different data sets. Other semiempirical models relating the reaeration rate to average velocity, slope of the energy gradient, and average depth include Churchill, Elmore, and Buckingham<sup>16</sup> and Bennett-Rathbun.<sup>15</sup> These predictive models have the following form, which is very similar to the semiempirical models discussed above:

$$K_2 \propto \frac{\bar{V}^a S^c}{H^b} \quad (14)$$

Table 1  
Empirical Prediction Models

$$K_2 \propto \frac{\bar{V}^a}{H^b}$$

	<u>a</u>	<u>b</u>
O'Connor-Dobbins (theory-based)	0.50	1.50
Bennett-Rathbun	0.607	1.689
Churchill, Elmore, and Buckingham	0.969	1.673
Langbein and Durum	1.00	1.33
Bansal	0.60	1.40

Table 2  
Semiempirical Prediction Models

	<u>a</u>	<u>b</u>
Krenkel-Orlob	0.408	0.660
Tsivoglou-Wallace	1.000	0
Cadwallader-McDonnell	0.500	1.000

where the coefficients  $a$ ,  $b$ , and  $c$  are 2.695, 3.085, and -0.823, respectively, for the Churchill et al. equation and 0.413, 1.408, and 0.273, respectively, for the Bennett-Rathbun equation.

#### Remarks

30. It is very difficult if not impossible to apply the theories of gas transfer to real situations. It is most difficult to determine the appropriate values for the coefficients or other parameters used by these concepts. The same is true for most numerical models. As mentioned for the O'Connor-Dobbins model, values for the surface renewal coefficient and the thin film thickness are not easily ascertained. Rathbun,<sup>5</sup> Zogorski and Faust,<sup>21</sup> and Lau<sup>22</sup> have presented a state-of-the-art review and evaluation of most techniques used to determine reaeration coefficients.

31. Some of the predictive models use average velocity and depth; if the hydraulic conditions are constant for the stream or channel reach, then these equations can be used. In most hydraulic structures, the hydraulic conditions change radically through the structure, and the concepts of average velocity and average depth cannot be easily applied.

## PART III: METHODOLOGY

### Alternatives to the Tracer Technique

32. Upstream and downstream DO contents can be used to compute the reaeration rate coefficient by performing a DO balance as developed by Streeter and Phelps.<sup>23</sup> This is accomplished by accounting for all the DO sources and sinks in the stream reach except atmospheric reaeration. Thus the difference between upstream and downstream DO contents (after accounting for the sources and sinks) is attributable to reaeration.

33. Another method is the disturbed-equilibrium technique<sup>24,25</sup> developed at the Water Pollution Research Laboratory. This technique uses sodium sulfite and a catalyst (cobalt chloride) to chemically deoxygenate the water. By observing the DO uptake in the stream reach and assuming that other DO sources and sinks are constant during measurements, the reaeration coefficient can be computed. DO uptake measurements made while using this method are presented herein.

### Tracer Technique

34. The gaseous tracer method for determining reaeration uses three tracers simultaneously. Krypton-85 (kr-85), as a dissolved gas, is the tracer for DO; tritium, as tritiated water molecules, is the tracer for dispersion; rhodamine-WT fluorescent dye provides an accurate measure of the time of travel and indicates when to sample for the two radioactive tracers.

35. To understand the tracer method, the equivalence of two processes must be made clear. The absorption of atmospheric gases (primarily oxygen) into water and the desorption of tracer gas from water to the atmosphere are equivalent. In either case, the driving force for gas transfer is the difference between the partial pressures of the gas in the atmosphere and in the water. Henry's law<sup>9</sup> states that a gas will attain a saturation concentration in a liquid that is proportional to

the partial pressure of the gas in the overlying atmosphere. Thus, there is a force causing molecular diffusion of gas molecules into the liquid until this saturation concentration is attained equalizing the partial pressures in the liquid and the atmosphere. For oxygen, a measure of the strength of the force, called "saturation deficit,"  $D$ , is the difference between the oxygen concentration at the point of saturation,  $C_s$ , and the concentration of oxygen,  $C$ , which actually exists in the water or

$$D = (C_s - C)_{ox} \quad (15)$$

As long as the concentration of oxygen in the water is less than the saturation concentration, there will be a net movement of oxygen from the atmosphere to the water. This process usually recognized as a first order reaction process can be derived from Fick's law and is represented by

$$\frac{dD}{dt} = -K_{ox} D \quad (16)$$

where  $t$  is time and  $K_{ox}$  is the reaeration rate coefficient for flowing water. This equation simply states that the rate of change of the saturation deficit at any time is proportional to the deficit at that time, or the greater the deficit, the greater the reaeration. The magnitude of the proportionality constant,  $K_{ox}$ , is dependent particularly upon the intensity of turbulent mixing in the system.

36. If there were no factors other than turbulent mixing affecting the oxygen concentration, integrating Equation 16 would provide a means for determining the proportionality constant,  $K_{ox}$ , through the relationship

$$D = D_o e^{-K_{ox} t} \quad (17)$$

where

$D$  = saturation deficit at some later time,  $t$

$D_o$  = saturation deficit at some initial time ( $t = 0$ )

There are many chemical and biological processes which affect  $D$  in

natural systems, and therein lies the value of using the inert gas tracer method. The inert gas is not affected by chemical or biological processes.

37. The desorption process of krypton from the water is equivalent to the absorption process of oxygen from the atmosphere. The driving force in the desorption of the tracer gas is the difference between the partial pressure of the krypton in the water and the partial pressure of the krypton in the atmosphere. For all practical purposes, the partial pressure and thus the concentration of krypton in the atmosphere is zero. Therefore, tracer gas in the water will be steadily lost to the atmosphere. A measure of the strength of the force causing gas loss is simply the concentration of tracer gas in the water. This process can be represented by

$$C = C_o e^{-K_{kr} t} \quad (18)$$

where

$C$  = concentration of kr-85 remaining in the water at some later time,  $t$

$C_o$  = concentration of kr-85 at some initial time ( $t = 0$ )

$K_{kr}$  = gas exchange coefficient for krypton in flowing water

Since krypton gas is inert, it is not subject to the chemical and biological processes that affect oxygen. This fact makes it possible to compute, through Equation 18, a gas exchange coefficient for krypton,  $K_{kr}$ , which reflects only the turbulent mixing process and direct physical gas transfer.

38. It has been shown that the ratio of exchange coefficients for these two gases is equal to a constant,<sup>1</sup> that is,

$$\frac{K_{kr}}{K_{ox}} = 0.83 \quad (19)$$

where

$K_{kr}$  = exchange coefficient for krypton

$K_{ox}$  = exchange coefficient for oxygen

This relationship is not affected by temperature (within the range of interest), degree of turbulent mixing, or the direction of gas transfer.

This makes possible the calculation of  $K_{kr}$  from Equation 18 and subsequent determination of  $K_{ox}$  with Equation 19.

39. Consider two points A and B which lie on a natural system such as a stream or channel. Let A be the upstream point and let a quantity of dissolved krypton gas be introduced upstream of A. If the tracer gas were introduced uniformly across the cross-sectional flow area and there were no vertical or horizontal velocity gradients in the flow causing dispersion, and if there were no tributaries to cause dilution, then the exchange coefficient of krypton-85,  $K_{kr}$ , between points A and B could be calculated from Equation 18 in the form

$$\frac{C_B}{C_A} = e^{-K_{kr}t} \quad (20)$$

where

$C_A, C_B$  = krypton-85 gas concentrations at A and B  
 $t$  = time of travel from A to B

40. However, since dilution and dispersion are present, they must be considered. Even if it were possible, direct measurement of dispersion and dilution is not necessary; a correction may be applied to Equation 20 by using the second radioactive tracer, tritium.

41. Tritium, in the form of tritiated water molecules, is released simultaneously with the krypton gas. The tritium concentration decreases from point A to point B since it is subjected to the dispersion and dilution of the reach. Thus, it provides an accurate measure of the dispersion and dilution. Since the tritium is in the form of tritiated water molecules, it is not adsorbed on the channel bottom or sides or otherwise lost in any significant amount. Because the tracers are released simultaneously the krypton-85 undergoes the same dispersion and dilution as the tritiated water.

42. The observed concentrations of tritium therefore provide an accurate correction for the effects of dispersion and dilution which can be applied to the krypton-85 gas concentrations, and the krypton exchange coefficient,  $K_{kr}$ , can be calculated by

$$\frac{\left(\frac{C_{kr}}{C_H}\right)_B}{\left(\frac{C_{kr}}{C_H}\right)_A} = e^{-K_{kr}t} \quad (21)$$

where

$$\left(\frac{C_{kr}}{C_H}\right)_A, \left(\frac{C_{kr}}{C_H}\right)_B = \text{ratios of krypton concentrations to tritium concentrations at points A and B}$$

t = time of travel from A to B

Decreases in tracer concentrations due to natural decay need not be considered since the isotopes' half-lives are usually much greater than the travel time.

#### Model Facility

43. The model used in this study was a 1:20-scale simulation of a single bay of the Lower Monumental Dam spillway located on the Snake River in Oregon. The model was designed and constructed for hydraulic similitude based on Froudian criteria. It reproduced a short portion of forebay and a single bay of the spillway section of the dam with the tainter gate for flow control. The stilling basin and a portion of the exit channel were included in the model (Figure 4).

44. The two spillway configurations tested were with and without a flip lip on the spillway face (Figure 5). The flip lip deflected flow along and near the surface of the tailwater (Figure 6) instead of allowing the water to plunge to the bottom of the stilling basin (Figure 7). This subjects the air-entrained flow to less pressure and greater exposure to the atmosphere which results in greater opportunity for gas transfer. The flip lip was located at el 132.28\* which was below the tailwater surface for the flow which was tested.

---

\* All elevations (el) cited herein are in metres referred to mean sea level.

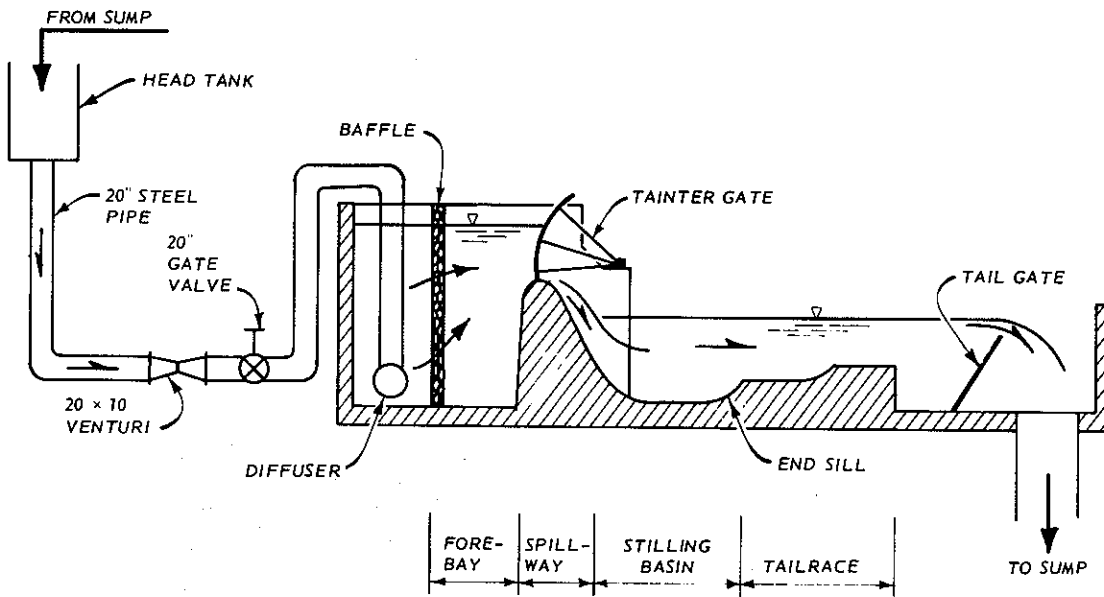


Figure 4. Model facilities

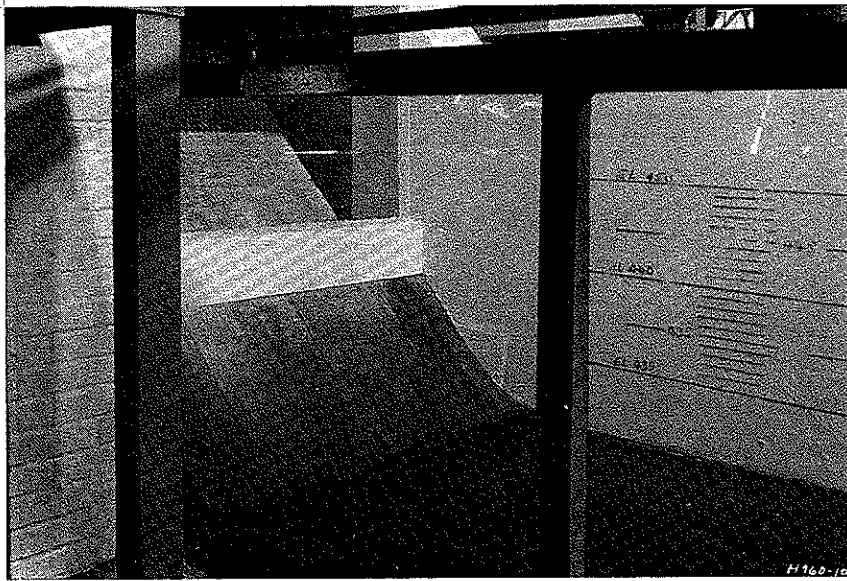
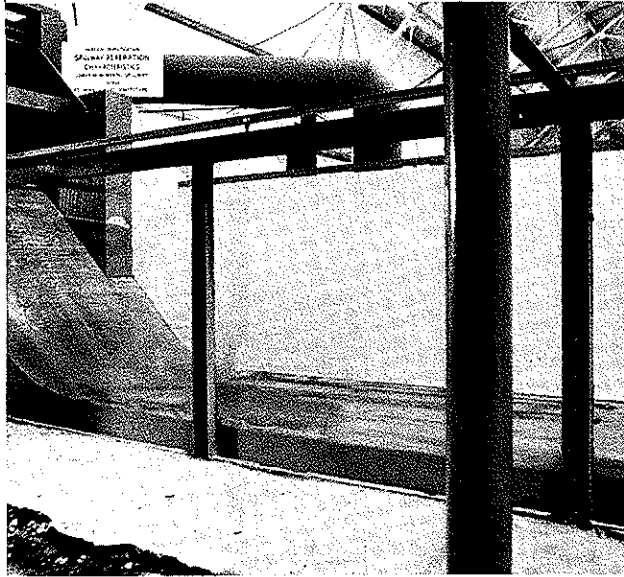


Figure 5. Spillway face without (top) and with (bottom) flip lip

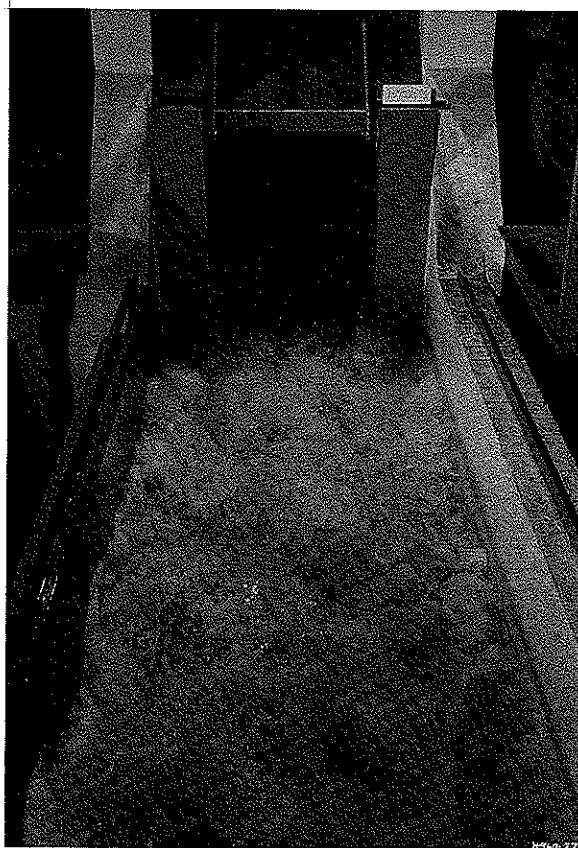
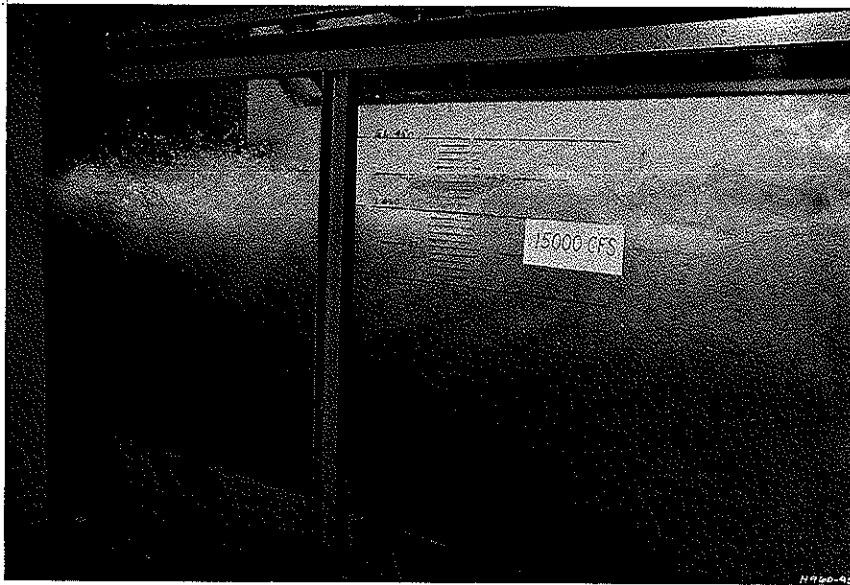


Figure 6. Flow conditions with flip lip  
(15,000 cfs = 425 cms)

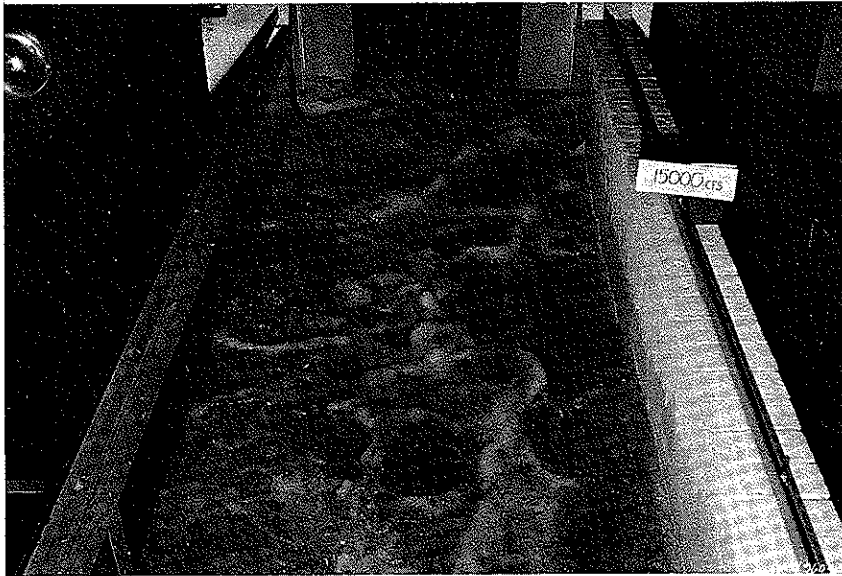
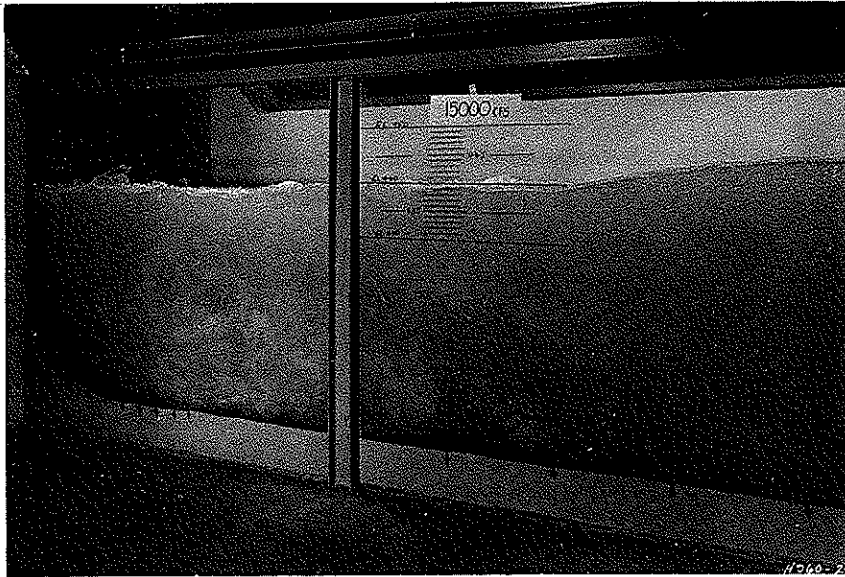


Figure 7. Flow conditions without flip lip  
(15,000 cfs = 425 cms)

45. Water was supplied to the model by a 51-cm-diameter pipe with a gate valve and measured with a venturi meter. The flow rate for all tests was 0.238 cms in the model which is equivalent to 425 cms in one bay of the prototype.

## PART IV: TESTING

### Apparatus and Equipment

46. Because of the short flow time through the model and quick passage of the dye cloud, previous sample collection methods<sup>2,3</sup> could not be used. A high speed sampling system was developed for use at both the upstream and downstream sampling stations (Figure 8). A submerged

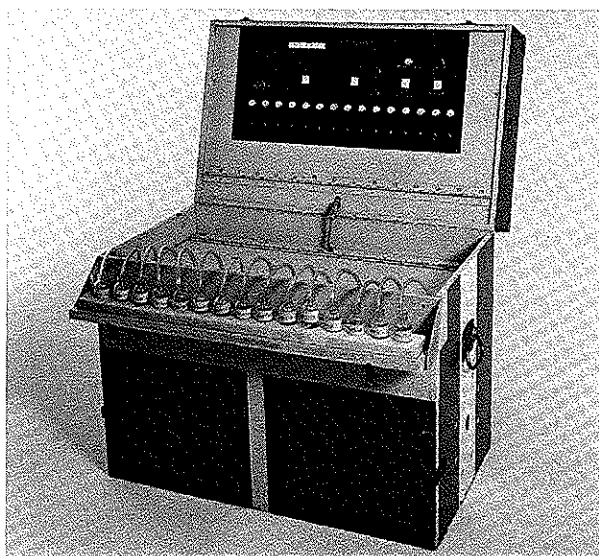


Figure 8. High speed sampling system

pump supplied water to a manifold which routed the flow to 15 sample bottles and a continuous flow fluorometer that was equipped with a recorder. Flow to the sample bottles and fluorometer was controlled with adjustable pinchcocks and was calibrated to a rate of 10 ml/sec. Electromechanical solenoid valves in the flow lines from the manifold to the sample bottles were used to shut off flow to the sample bottles at a prescribed time. Water was continuously supplied to the sample bottles and fluorometer. Excess water to the sample bottles was continuously spilled (Figure 9). As the dose passed the sampling station, part of it was pumped through the manifold to the sample bottles. The solenoid valves were closed, one at a time, at a prescribed interval,

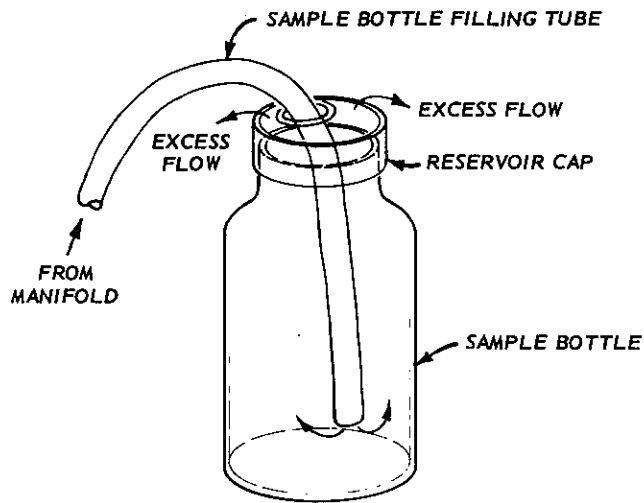


Figure 9. Sampling collection bottle

thereby shutting off the flow to each bottle and capturing a discrete sample in time. Figure 10 is a schematic of the sampling system. The two systems used in the upstream and downstream approaches were constructed to be identical, with the length and volume of all water-carrying tubing and parts minimized.

47. The flow was instantaneously dosed with the radioactive tracers and fluorescent dye by crushing the glass dose container with a "bottle-breaker." The dose container was "instantly" crushed by striking a plunger with a hammer.

#### Procedure

48. At the beginning of each test the model was checked for correct flow and water surface elevations and the hydraulic situation allowed to stabilize. The sampling systems which were located at the two sampling stations (Figure 11) were put into operation. Once the sampling systems, the fluorometers, and the strip chart recorder were ready, the flow was dosed with the tracer mixture (14.0 millicuries of krypton-85, 6.0 millicuries of tritium, and fluorescent dye) upstream of the model. Shortly after the leading edge of the dye cloud passed the upstream

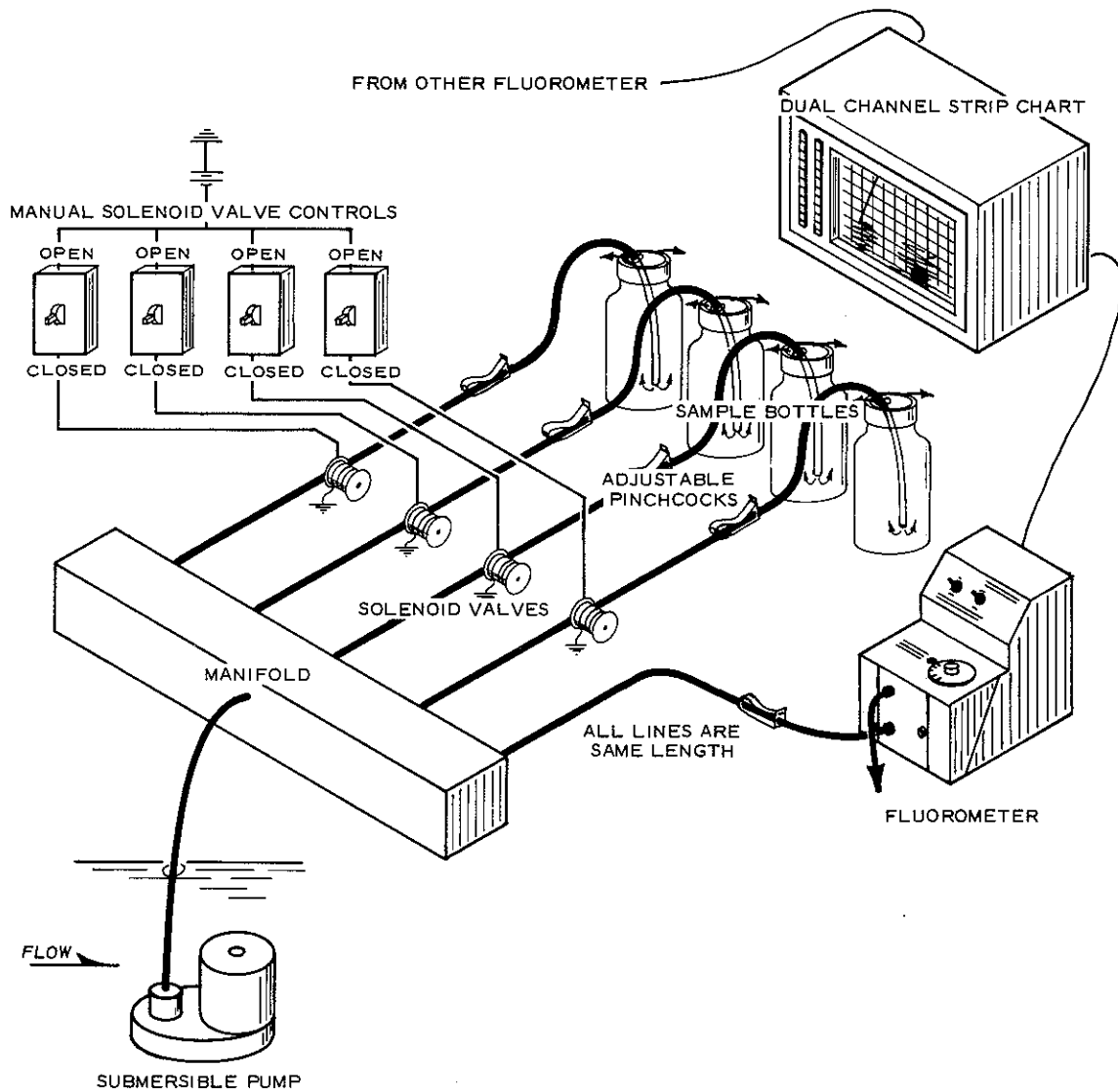


Figure 10. Sampling system schematic

sampling station (indicated by the fluorometer and recorder), sampling was initiated and marked on the chart of the recorder. A sample was taken every 2 sec. Every fifth sample was indicated on the chart to help assure analysis of the correct samples. The same procedure was followed as the dose passed the downstream sampling station.

49. As soon as the tracer cloud had passed and all fifteen samples had been collected, the bottle-filling tubes were carefully withdrawn, and the bottles were tightly capped and taped shut with

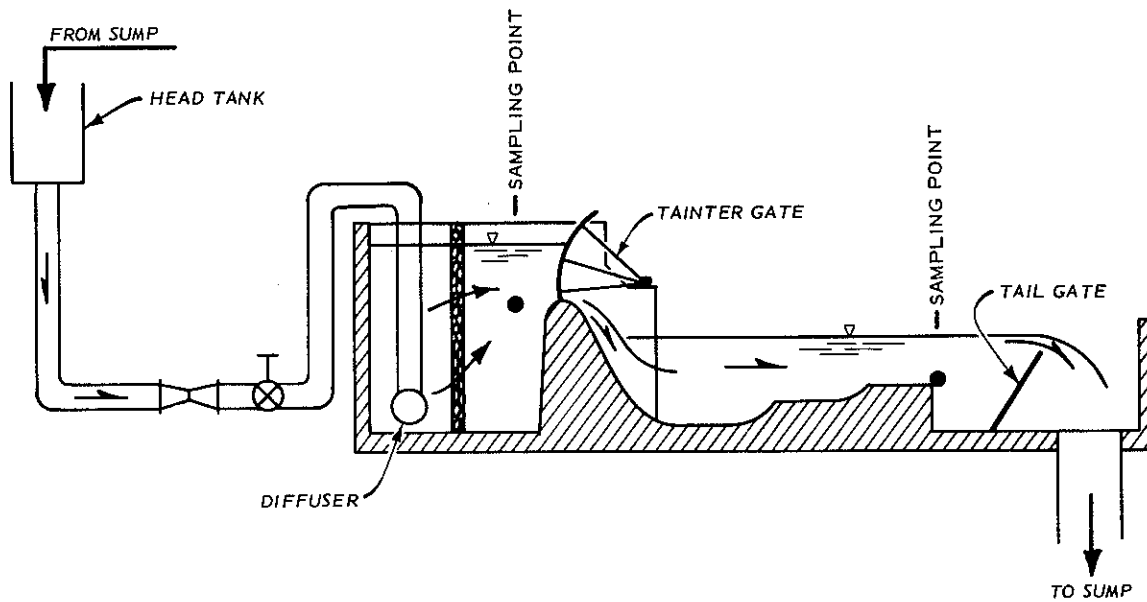


Figure 11. Sampling station location

electrical tape. The capped samples were submerged in water kept at a constant temperature for transport to the laboratory for analysis.

### Analysis

50. As has been stated, the fluorescent dye tracer was used to determine when the dose passed the sampling stations. With the sampling technique used in these tests, samples were taken over a large portion of the dye cloud assuring the collection of samples around the time of peak dye concentration and peak radioactive tracer content.

51. The travel time through the model was determined from the recorded fluorescent dye curves. From center-of-mass (upstream curve) to center-of-mass (downstream curve) could be considered as the travel time between the sampling stations. However, collecting samples for analysis near the center-of-mass of the dye cloud was not practical since the center-of-mass was indeterminable until after the dye cloud had passed the sampling station. Further, the krypton gas transfer coefficient,  $K_{kr}$ , computed with Equation 21 is only valid when used with the travel

time with which it was calculated. By examining Equation 21 it can be seen that the unknown in the equation is actually the product of  $K_{kr} t$ . Substituting any observed time of travel would result in a different exchange coefficient, but the product would remain the same.

52. For analytical purposes, the samples of principal interest were those taken when the tracers were at their peak concentrations. These samples were chosen by their location in time marked on the dye curve recordings (Figure 12). Usually four upstream and four downstream

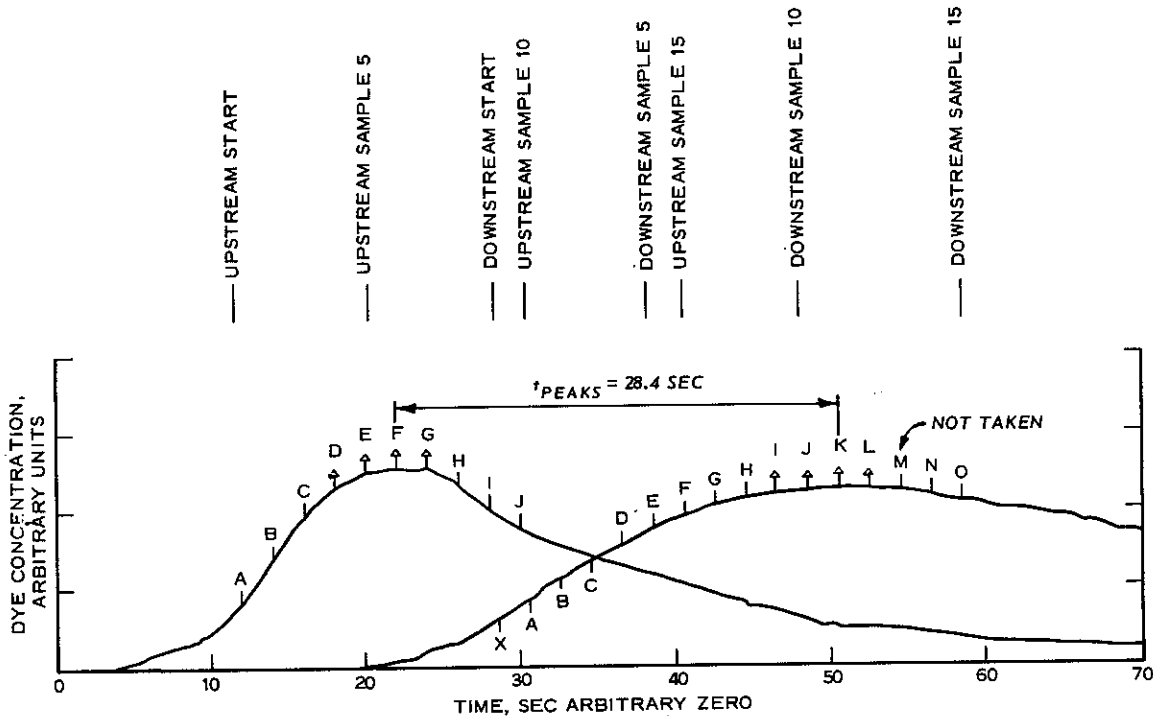


Figure 12. Dose IV dye curve

samples were analyzed for krypton and tritium content. If these two sets of samples were centered at their respective peaks, the average krypton-to-tritium ratio of each set and the lapse time from peak to peak were used to calculate  $K_{kr}$  (dose III). If a set of samples was centered off the peak, then only those samples centered around or near the peak were used to compute  $K_{kr}$ . In this case the temporal center of the samples used to compute  $K_{kr}$  was used to determine travel time (dose II).

53. Samples were then prepared for analysis using the method

described by Cohen, et al.<sup>26</sup> The krypton-85 and tritium concentrations were determined simultaneously in a Packard Tri-Carb liquid scintillation counter. Three replicates of each sample were prepared and cycled through three counting sequences to reduce the effect of analytical error.

#### DO Uptake Tests

54. After the tracer tests had been completed, tests for DO uptake using the disturbed equilibrium technique were conducted in the hydraulic model. Under similar flow and design conditions as previously described, a sodium sulfite and catalyst solution was injected into the flow upstream of the model. The chemicals combined with free oxygen, effectively creating an oxygen deficit in the water. The flow was re-aerated as it passed through the model thus decreasing the oxygen deficit.

55. DO concentrations were measured at the same sampling points as in the radioactive tracer studies. A standard YSI DO probe was used to determine the DO content. In addition, a modified Winkler titration technique was employed to spot-check measurements.

## PART V: RESULTS

56. Table 3 presents krypton-to-tritium ratios for the four tracer tests. Doses I and II were the tests with the flip lip; doses III and IV were the tests without the flip lip. The ratios whose samples were centered around or closest to the dye peaks were used in the analysis for  $K_{kr}$ . The time of flow was determined by the location of these samples on the dye curves. Plates 1-4 show the dye curves and temporal locations at samples. The time of flow for each dose, which was used in computing the exchange coefficient  $K_{kr}$ , is marked "best" on these plates. Plates 5-8 show krypton-to-tritium ratios versus time on a semilog coordinate system. The slope of the line is the krypton gas exchange coefficient.

57. Table 4 shows the samples whose krypton-to-tritium ratios were used to calculate  $K_{kr}$  for each dose. The travel times associated with these "best" samples are also presented. By applying Equation 19 the exchange coefficient for oxygen  $K_{ox}^T$  at the ambient water temperature  $T(^{\circ}C)$  was computed. Applying a correction for temperature, the reaeration rate coefficient for oxygen at  $20^{\circ}C$  was determined by the following equation:

$$K_{ox}^{20} = K_{ox}^T 1.022^{(20-T)} \quad (22)$$

The krypton gas fraction remaining in the water at the downstream station was computed by

$$F. R. = \frac{\bar{r}_{downstream}}{\bar{r}_{upstream}}$$

where

F. R. = fraction remaining

$\bar{r}_{upstream}$ ,  $\bar{r}_{downstream}$  = mean krypton-to-tritium ratio for "best" samples at the upstream and downstream station

Table 3  
Krypton-to-Tritium Ratios for All Tests

<u>Upstream Station</u>		<u>Downstream Station</u>	
<u>Sample</u>	<u>kr-85/H-3</u>	<u>Sample</u>	<u>kr-85/H-3</u>
<u>Dose I</u>			
F	1.3415	G	0.8326
G	Not available	H	0.8464
H	1.3563	I	0.8413
I	1.3438	J	0.8005
<u>Dose II</u>			
D	1.2577	B	0.7854
E	1.2554	C	0.7486
F	1.2662	D	0.7338
G	1.3064	E	0.7314
<u>Dose III</u>			
F	1.3694	I	0.9364
G	1.3811	J	0.9189
H	1.3684	K	0.9471
I	1.3370	L	0.8966
<u>Dose IV</u>			
D	1.2585	I	0.9568
E	1.2650	J	0.9688
F	1.2712	K	0.9158
G	1.2765	L	0.9111

Table 4  
 Samples Used in  $K_{kr}$  Analysis and Travel Time

Dose	Samples Included		Travel time, t sec
	Upstream	Downstream	
I	F, H, I	I, J	22.7
II	F, G	B, C, D, E	24.5
III	F, G, H, I	I, J, K, L	28.5
IV	E, F, G	J, K, L	28.5

For example, the gas fraction remaining at the downstream station for dose I was

$$\frac{0.8209}{1.3472} = 0.6093$$

The gas fraction lost to the atmosphere was

$$1.000 - 0.6093 = 0.3907$$

Similar calculations were made for the remaining doses.

58. Table 5 summarizes the tracer tests. The flip lip increased the gas transfer by 37.2 percent and increased  $K_{ox}^{20^{\circ}C}$  by 80.6 percent. Travel time decreased by 17.2 percent.

59. During dose III, air bubbles which were entrained in the water were being pumped through the sampling system. To avoid possible loss of tracer gas in the samples due to these air bubbles, the pump was positioned slightly lower in the water prior to dose IV. Repositioning the pump may have caused the difference in gas loss for doses III and IV. This difference was larger than expected.

60. Figure 13 is a comparison of DO predicted with the  $K_2$  and t obtained from the tracer study and the DO observed in the disturbed equilibrium (DE) tests. The small variations about the perfect agreement line were probably due to incomplete chemical reactions in the DE tests or slight differences in the mixing conditions in the model for the DE tests and tracer tests.

Table 5  
Test Summary

<u>Design</u>	<u>Dose</u>	<u>Travel Time sec</u>	<u>Fraction of Gas Lost</u>	<u>Water Tempera- ature °C</u>	<u>K<sub>ox</sub><sup>20°C</sup> per hr</u>
With flip lip	I	22.7	0.3907	29.5	77.0
With flip lip	II	24.5	0.4171	29.5	77.7
Mean		23.6	0.4039		77.3
Without flip lip	III	28.5	0.3220	30.5	47.1
Without flip lip	IV	28.5	0.2667	29.5	38.4
Mean		28.5	0.2944		42.8

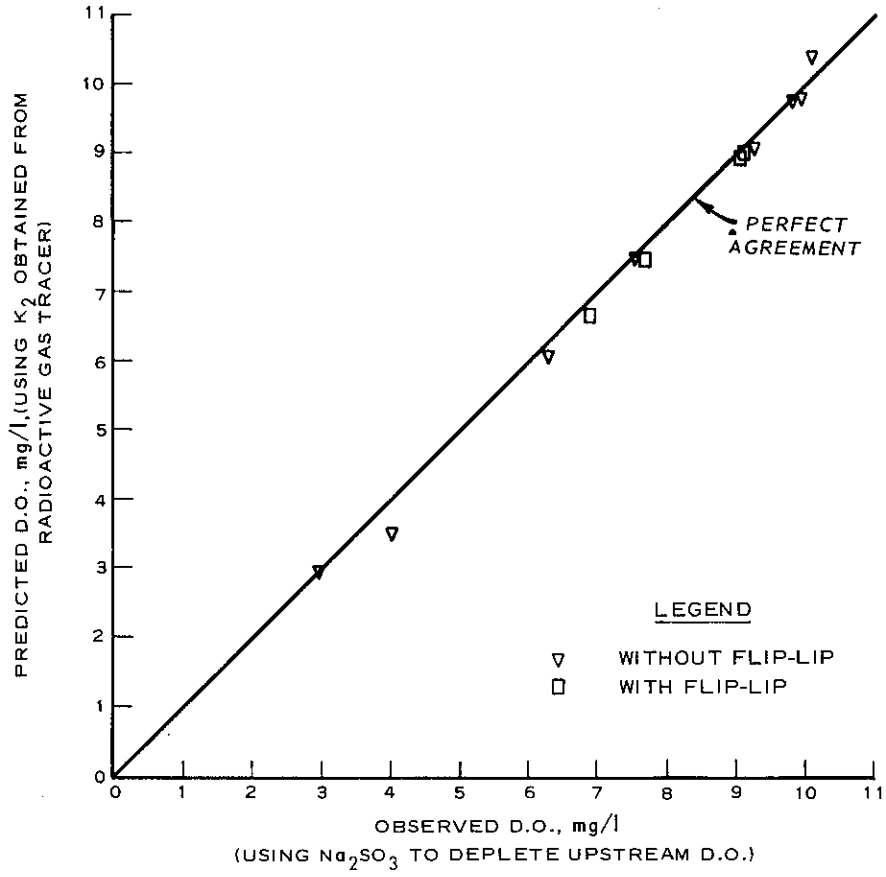


Figure 13. Predicted DO versus observed DO.

## PART VI: CONCLUSIONS

61. The tests showed that the krypton-85/tritium tracer technique was applicable to a model of a hydraulic structure for determining the gas transfer characteristics of a particular model design. The technique provided excellent reproducibility as indicated by the small variation in results from replicate tests. The technique was demonstrated to be sufficiently sensitive to be used as a tool for a qualitative comparison of the gas transfer of the different designs tested. However, the technique may not be sensitive to more subtle differences. The hydraulic model which was tested had very turbulent hydraulic conditions and large discharge compared to other hydraulic models. Thus, there may exist a threshold below which sufficient gas transfer does not occur to permit detection.

62. A comparison of DO observed in the sodium sulfite tests and predicted DO based on the tracer tests was quite favorable (Figure 13). Thus, either technique would provide adequate information on gas transfer for this particular model and these design changes. The sensitivity threshold for the DE technique may be different from the tracer technique threshold because of the different measurement and analysis techniques employed. Further testing is necessary to evaluate the techniques in greater depth.

63. In a recirculating water supply system such as that used at the model facility described, contamination of water entering the model with water containing chemicals is possible. It is therefore imperative that the circulation time be much greater than the time required for data collection. The sodium sulfite technique is not feasible if the model is large such that the discharge is greater than 0.25 cms, since large quantities of sodium sulfite solution must be prepared for the high injection rate necessary for this large flow.

## PART VII: RECOMMENDATIONS

64. It is recommended that this type of model study be conducted for projects (proposed or existing) where modifications are contemplated to improve gas transfer. A qualitative evaluation of different structural alternatives may result in a more effective or economical design. It is probable that prototype response is directly related to changes in gas transfer characteristics observed in a model. However, relationships for quantitative transfer of gas exchange characteristics from model to prototype have not been developed yet. Increased gas exchange in a model directly indicates greater oxygen transfer to low DO water in a prototype. Increased gas exchange in the model should indicate decreased supersaturation if the prototype causes supersaturation. It is also recommended that similar tests be conducted in hydraulic models that range in size and scale to determine the gas transfer occurring in other hydraulic models and determine the effects of other models on the applicability of the technique. Other types of simple geometry should be tested to provide a basis for scaling criteria and to evaluate detection thresholds below which the technique is not adequate.

65. Research to determine scaling relationships should be conducted using physical models of simple turbulent flow systems. A parameterization study to isolate and evaluate the significant parameters affecting the scaling of gas transfer in models should be conducted. Theory, applicable to scaling gas transfer, should be developed concurrently with the parameterization study. Thus an interface is provided for evaluating experimental and theoretical results. This approach is being pursued at the Waterways Experiment Station in research funded by the Environmental and Water Quality Operational Studies. It is hoped that this will result in a method of estimating scale relationships between the gas transfer characteristics of a model and prototype and the prediction of oxygen uptake in the prototype.

## REFERENCES

1. Tsivoglou, E. C., et al., "Tracer Measurements of Atmospheric Reaeration: I. Laboratory Studies," Journal, Water Pollution Control Federation, Vol 37, No. 10, Oct 1965.
2. Tsivoglou, E. C., et al., "Tracer Measurements of Stream Reaeration: II. Field Studies," Journal, Water Pollution Control Federation, Vol 40, No. 2, Feb 1968.
3. Tsivoglou, E. C., and Wallace, J. R., "Characterization of Stream Reaeration Capacity," EPA-R3-72-012, 1972, U. S. Environmental Protection Agency.
4. Tsivoglou, E. C., "Tracer Measurement of Stream Reaeration," 1967, Federal Water Pollution Control Administration.
5. Rathbun, R. E., "Reaeration Coefficients of Streams -- State-of-the-Art," Hydraulics Journal, American Society of Civil Engineers, Vol 103, No. HY4, Apr 1977.
6. Daily, J. W., and Harleman, D. R. F., Fluid Dynamics, Addison-Wesley, 1973.
7. Einstein, A., "Investigations on the Theory of Brownian Movement... Assisted with Notes by R. Furth" (translated by A. D. Cowper). Methuen, London 1927, reprinted by Dover, New York, 1956.
8. Stokes, G. G., "On the Effects of the Internal Friction of Fluids on the Motion of Pendulums," Cambridge Philosophical Society, Transactions, Vol 1X, Part II, 1850.
9. Schroeder, E. D., Water and Wastewater Treatment, McGraw-Hill, New York, 1977.
10. LeMehaute B., An Introduction to Hydrodynamics and Water Waves, Springer-Verlag, 1976.
11. Lewis, W. K., and Whitman, W. C., "Principles of Gas Absorption," Industrial and Engineering Chemistry, Vol 16, No. 12, 1924, pp 1215, 1220.
12. Danckwerts, P. V., "Significance of Liquid-Film Coefficient in Gas Absorption," Industrial and Engineering Chemistry, Vol 43, No. 6, 1951, pp 1460, 1467.
13. Dobbins, W. E., "The Nature of the Oxygen Transfer Coefficient in Aeration Systems," Proceedings, Manhattan College Conference on Biological Waste Treatment, New York, 1955.

14. O'Connor, D. J., and Dobbins, W. E., "Mechanism of Reaeration in Natural Streams," Transactions, American Society of Civil Engineers, Vol 123, 1958.
15. Bennett, J. P., and Rathbun, R. E., "Reaeration in Open-Channel Flow," U. S. Geological Survey Open-File Report, Apr 1971, Bay St. Louis, Miss.
16. Churchill, M. A., Elmore, H. L., and Buckingham, R. A., "The Prediction of Stream Reaeration Rates," Journal, Sanitary Engineering Division, American Society of Civil Engineers, Vol 88, No. SA4, Proc. Paper 3199, July 1962, pp 1-46.
17. Langbein, W. B., and Durum, W. H., "The Aeration Capacity of Streams," U. S. Geological Survey Circular No. 542, 1967, Reston, Va.
18. Bansal, M. K., "Atmospheric Reaeration in Natural Streams," Water Research, Pergamon Press, Oxford, England, Vol 7, No. 5, May 1973, pp 769-782.
19. Krenkel, P. A., and Orlob, G. T., "Turbulent Diffusion and the Reaeration Coefficient," Transactions, American Society of Civil Engineers, Vol 128, Part III, Paper No. 3491, 1963, pp 293-334.
20. Cadwallader, T. E. and McDonnell, A. J., "A Multivariate Analysis of Reaeration Data," Water Research, Great Britain, Vol 3, 1969, pp 731-742.
21. Zogorski, J. S., and Faust, S. D., "Atmospheric Reaeration Capacity of Streams, Part I: Critical Review of Methods Available to Measure and to Calculate the Atmospheric Reaeration Rate Constant," Environmental Letters, Vol 4, No. 1, 1973.
22. Lau, Y. L., "A Review of Conceptual Models and Prediction Equations for Reaeration in Open-Channel Flow," Technical Bulletin, No. 61, 1972, Inland Waters Branch, Canadian Department of the Environment.
23. Streeter, H. W., and Phelps, E. B., "A Study of the Pollution and Natural Purification of the Ohio River," Public Health Bulletin No. 146, 1925, U. S. Public Health Service, Washington, D. C.
24. Edwards, R. W., Owens, M., and Gibbs, J. W., "Estimates of Surface Aeration in Two Streams," Journal, Institution of Water Engineers, London, England, Vol 15, No. 5, Aug 1961, pp 395-405.
25. Gameson, A. L. H., Truesdale, G. A., and Downing, A. L., "Reaeration Studies in a Lakeland Beck," Journal, Institution of Water Engineers, London, England, Vol 9, No. 7, Nov 1955, pp 571-594.

26. Cohen, J. B., et al., "Analytical Method for the Determination of  $^3\text{H}$  and  $^{85}\text{Kr}$  in Aqueous Samples by Liquid Scintillation Techniques," Talanta, 1968.

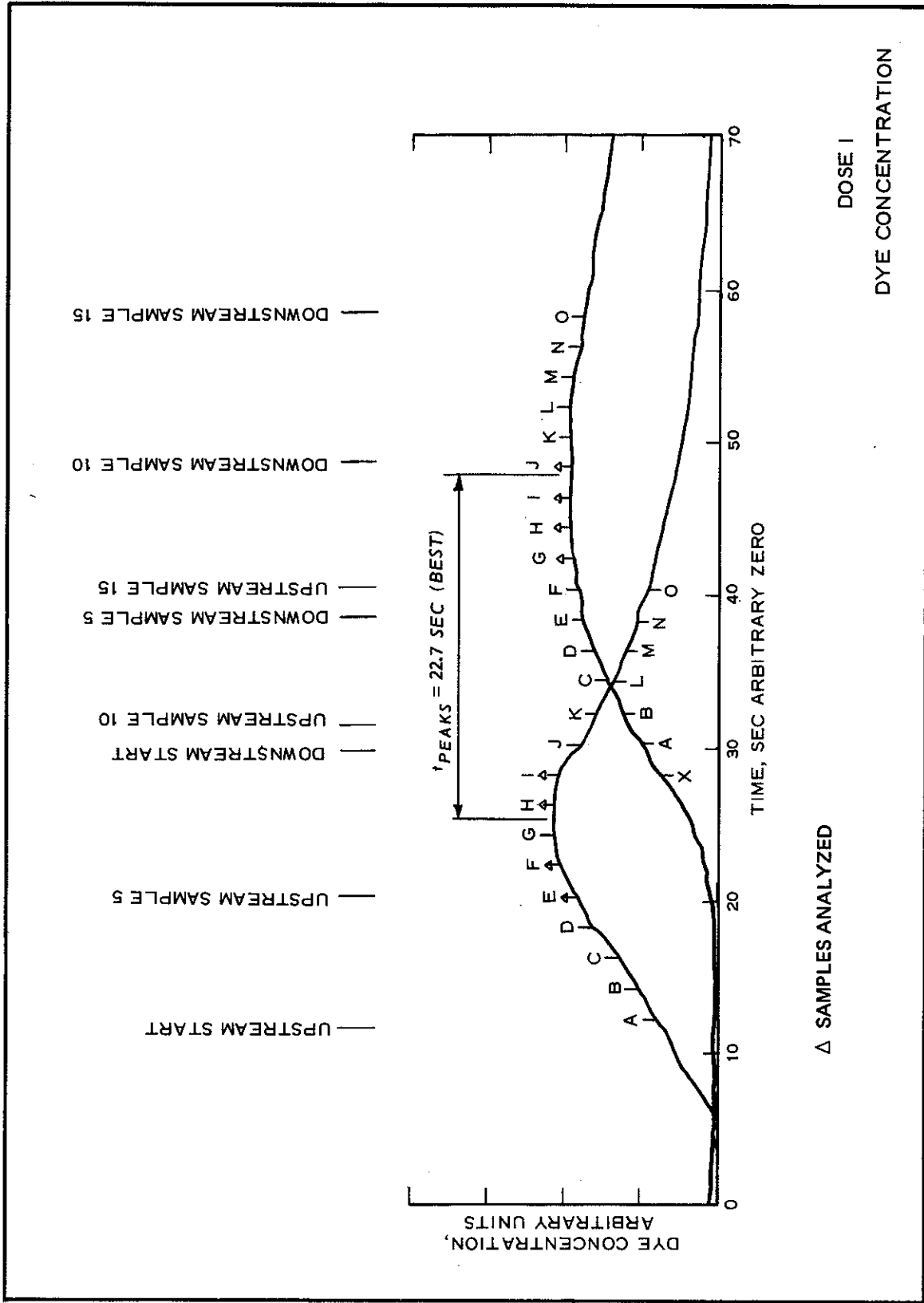
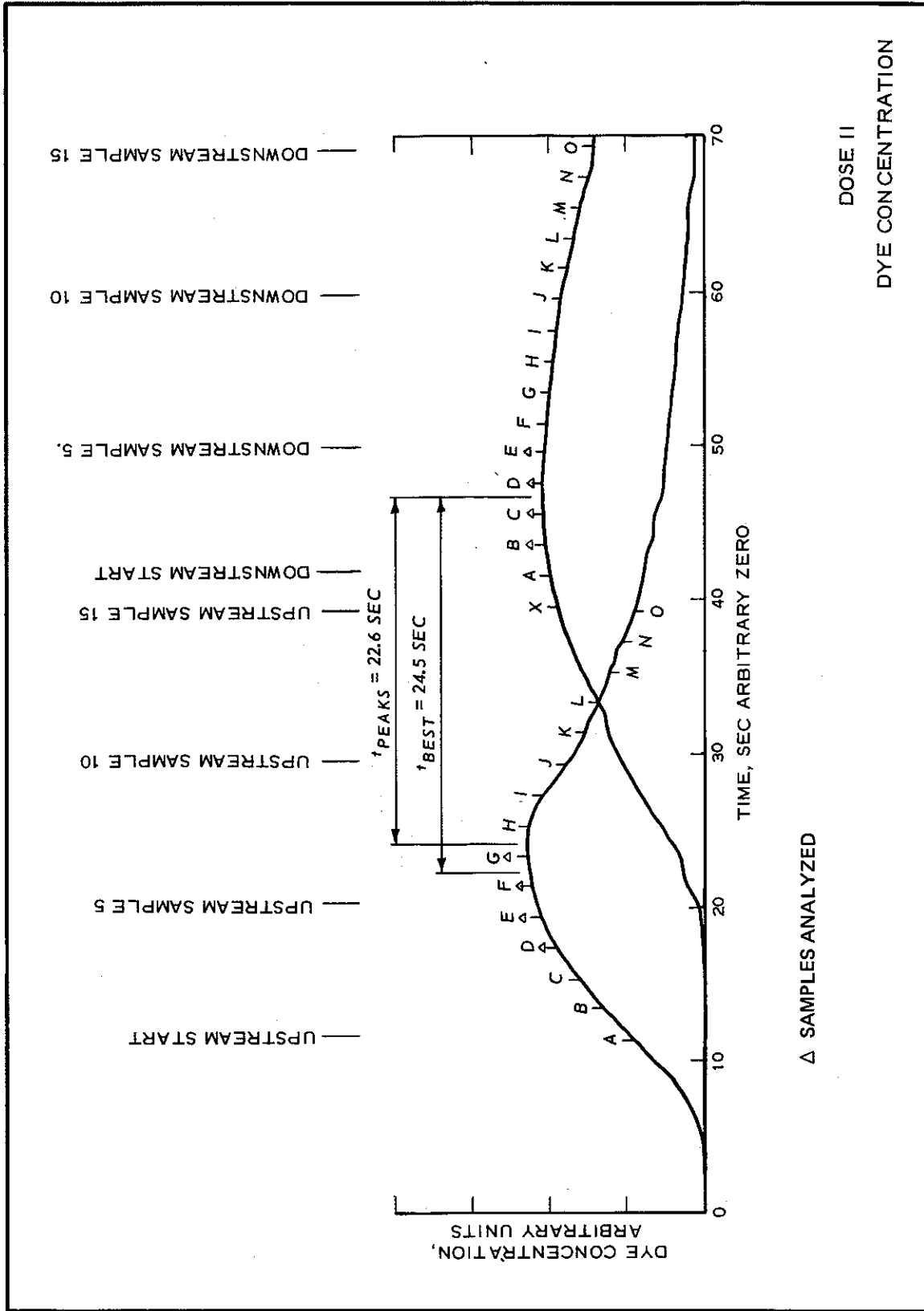


PLATE 1



DOSE II  
DYE CONCENTRATION

Δ SAMPLES ANALYZED

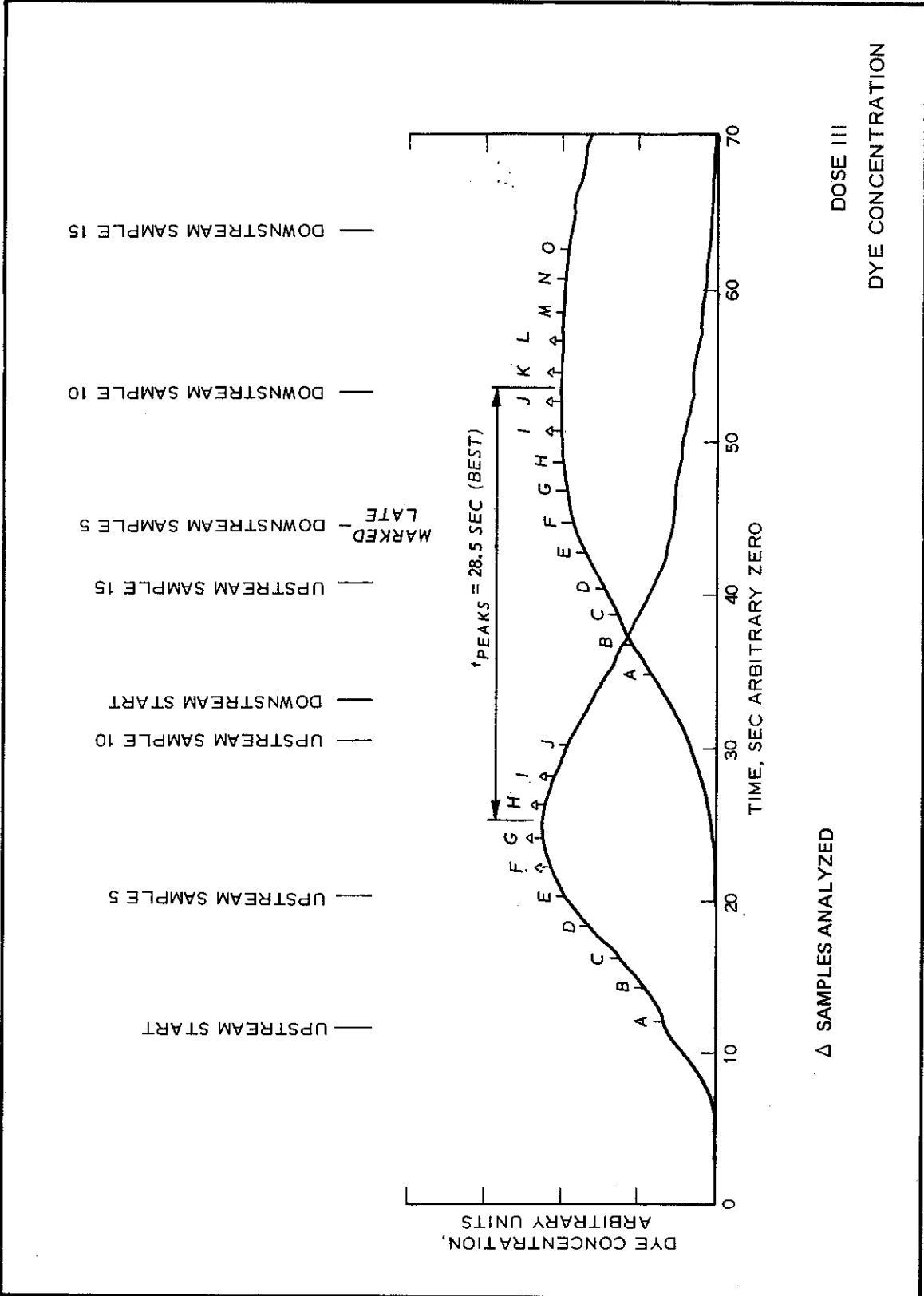
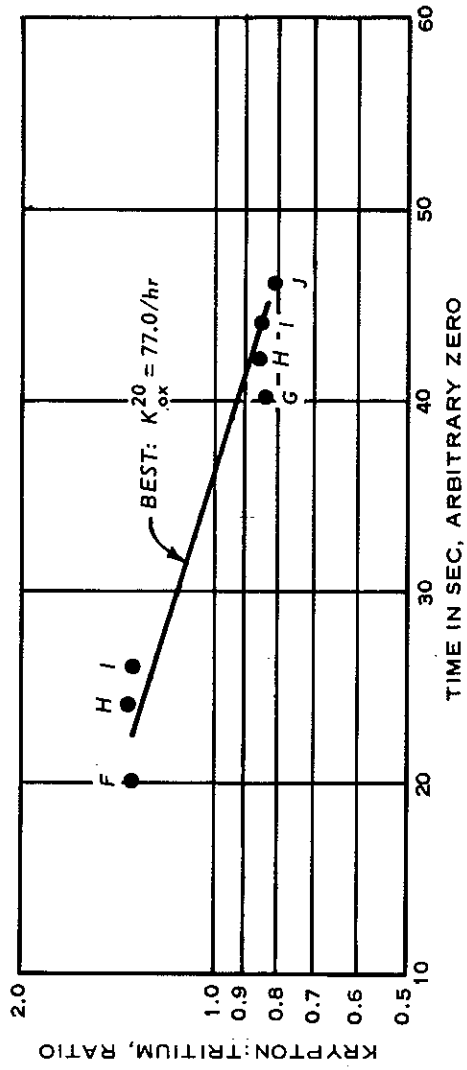
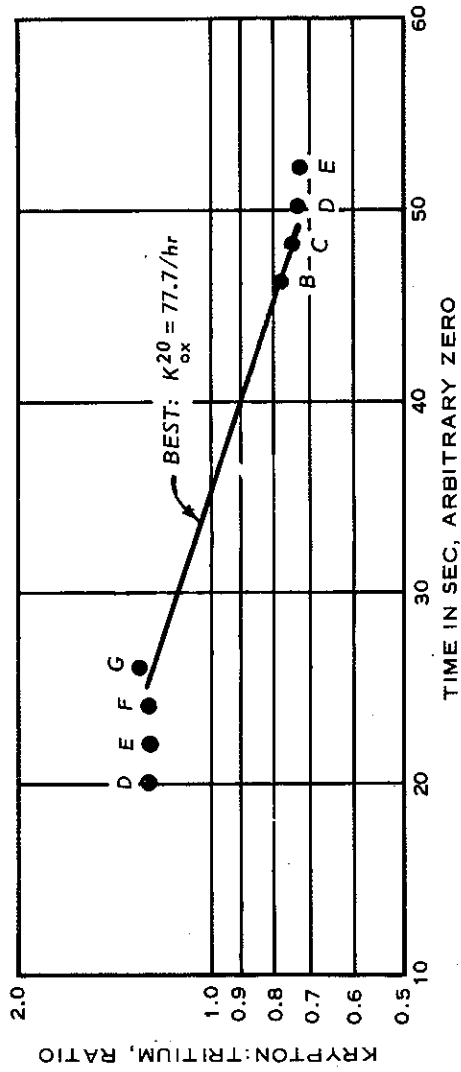


PLATE 3



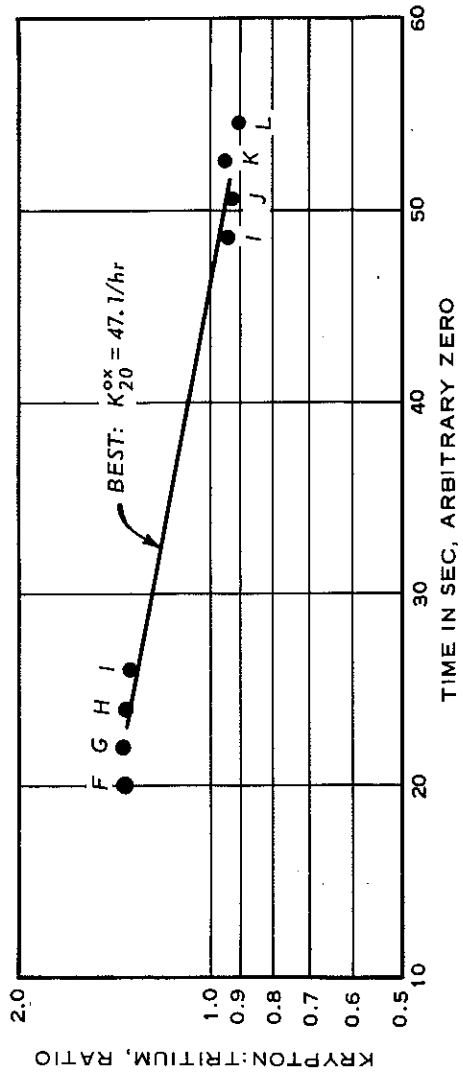


DOSE I  
(Kr:H<sub>3</sub>) VERSUS TIME

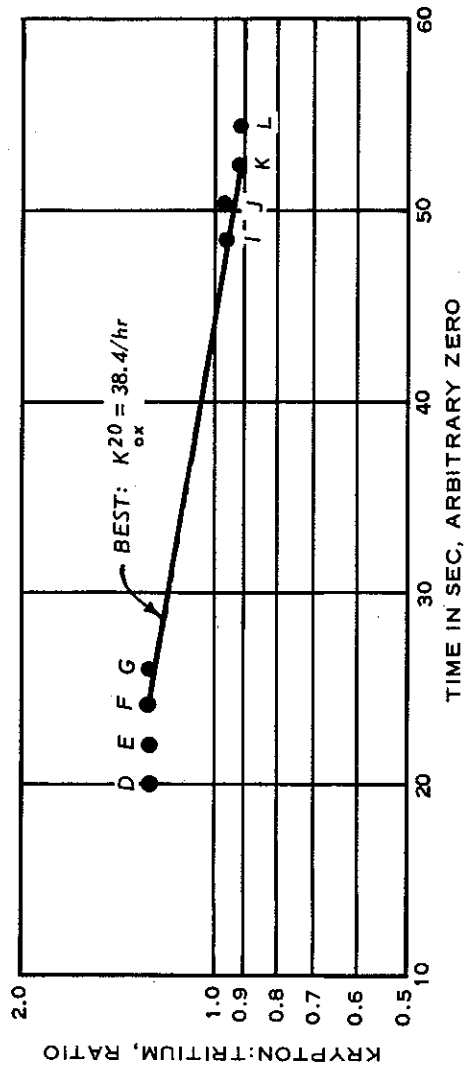


DOSE II  
(Kr:H<sub>3</sub>) VERSUS TIME

Small vertical text on the right edge of the page, likely a page number or reference code.



DOSE III  
(Kr:H<sub>3</sub>) VERSUS TIME



DOSE IV  
(Kr:H<sub>3</sub>) VERSUS TIME

In accordance with letter from DAEN-RDC, DAEN-ASI dated 22 July 1977, Subject: Facsimile Catalog Cards for Laboratory Technical Publications, a facsimile catalog card in Library of Congress MARC format is reproduced below.

Wilhelms, Steven C

Tracer measurement of reaeration: Application to hydraulic models; hydraulic model investigation / by Steven C. Wilhelms. (Hydraulics Laboratory. U.S. Army Engineer Waterways Experiment Station) ; prepared for Office, Chief of Engineers, U.S. Army, under CWIS 31042, (EWQOS Work Unit 31604 (IIIA.2) -- Vicksburg, Miss. : U.S. Army Engineer Waterways Experiment Station; Springfield, Va. : available from NTIS, 1981.

43 p., [4] leaves of plates : ill. ; 27 cm. (Technical report / U.S. Army Engineer Waterways Experiment Station ; E-80-5)

Cover title.

"December 1980."

References: p. 41-43.

1. Hydraulic models. 2. Radioactive tracers. 3. Reaeration. 4. Tracers. I. United States. Army. Corps of Engineers. Office of the Chief of Engineers. II. United States. Army Engineer Waterways Experiment Station. Hydraulics Laboratory. III. Title. IV. Series: Technical report (United States. Army Engineer Waterways Experiment Station) ; E-80-5.  
TA7.W34 no.E-80-5